Published in final edited form as:
Prostate. 2014 April ; 74(4): 346–358. doi:10.1002/pros.22751.

Prostate Angiogenesis in Development and Inflammation

Letitia Wong[1,2], **Jerry Gipp**[1], **Jason Carr**[1], **Christopher Loftus**[1], **Molly Benck**[1], **Sanghee Lee**[1], **Vatsal Mehta**[3], **Chad Vezina**[3], and **Wade Bushman**[1,*]

[1]Department of Urology, University of Wisconsin School of Medicine and Public Health, Madison, Wisconsin

[2]Molecular and Environmental Toxicology Center, University of Wisconsin School of Medicine and Public Health, Madison, Wisconsin

[3]Department of Comparative Biosciences, University of Wisconsin-Madison, Madison, Wisconsin

Abstract

BACKGROUND—Prostatic inflammation is an important factor in development and progression of BPH/LUTS. This study was performed to characterize the normal development and vascular anatomy of the mouse prostate and then examine, for the first time, the effects of prostatic inflammation on the prostate vasculature.

METHODS—Adult mice were perfused with India ink to visualize the prostatic vascular anatomy. Immunostaining was performed on the E16.5 UGS and the P5, P20 and adult prostate to characterize vascular development. Uropathogenic *E. coli* 1677 was instilled transurethrally into adult male mice to induce prostate inflammation. RT-PCR and BrdU labeling was performed to assay anigogenic factor expression and endothelial proliferation, respectively.

RESULTS—An artery on the ventral surface of the bladder trifurcates near the bladder neck to supply the prostate lobes and seminal vesicle. Development of the prostatic vascular system is associated with endothelial proliferation and robust expression of pro-angiogenic factors Pecam1, Tie1, Tek, Angpt1, Angpt2, Fgf2, Vegfa, Vegfc, Figf. Bacterial-induced prostatic inflammation induced endothelial cell proliferation and increased vascular density but surprisingly decreased pro-angiogenic factor expression.

CONCLUSIONS—The striking decrease in pro-angiogenic factor mRNA expression associated with endothelial proliferation and increased vascular density during inflammation suggests that endothelial response to injury is not a recapitulation of normal development and may be initiated and regulated by different regulatory mechanisms.

Keywords

Prostate; Vasculature; Inflammation; Development

INTRODUCTION

The prostate is an androgen-dependent male accessory sex organ that is composed of the epithelial ductal glands surrounded by the stromal components, including the vasculature. In addition to androgen stimulation, the prostate requires nutrients and oxygen supplied by the vasculature for normal development, growth and function. Studies of the adult rat prostatic gland have consistently emphasized the importance of the prostatic vascular system in

*Correspondence to: Dr. Wade Bushman, MD, PhD, Department of Urology, University of Wisconsin School of Medicine and Public Health, K6/562 Clinical Sciences Center, 600 Highland Avenue, Madison, WI 53792. bushman@urology.wisc.edu.

growth homeostasis, yet its aspect in prostate biology is still understudied. In response to androgen deprivation, there was an early and rapid reduction in blood flow to the adult rat ventral prostate after castration accompanied with vasoconstriction, increased vascular permeability, increased apoptosis and decreased proliferation of endothelial cells that occurred prior to the onset of prostatic epithelial cell apoptosis and tissue regression [1–7]. Androgen supplements rapidly restored the prostatic vasculature after castration that was required for the subsequent epithelial regeneration [1,2,4]. Studies in human prostates have further revealed vascular changes in prostate cancer and benign prostatic hyperplasia (BPH) including increased vessels with tiny lumens and irregular shapes, increased vessel density, and reduced blood flow, suggesting changes in vascular architecture or anatomy may have a potential role in prostate diseases [8–11]. To date, there has been only one published study to describe the vascular anatomy in the rat ventral prostate [12]. The arterial supply to the ventral lobe of the adult rat prostate was shown to derive in common or individually from the inferior vesical artery. The arterioles and venules traveled along the periphery of the glandular lobules while thin walled capillaries predominated immediately adjacent to the basement membranes of the glands as well as within the stroma surrounding the ducts. As of yet, the vascular anatomy of the adult mouse prostate and the development of the mouse prostatic vascular system have never been studied.

Vascular remodeling is a critical feature during inflammation after tissue injury and is mediated by angiogenic factors [13–15]. Studies in rodents infected with the respiratory pathogen *Mycoplasma pulmonis* have showed that bacterial infection induced airway inflammation was accompanied by numerous early vascular responses that preceded the tissue remodeling and was persistent as the infection continued toward chronic conditions [16]. The vascular remodeling in the trachea in response to bacterial infection involved increased endothelial cell proliferation, enhanced angiogenesis, increased vessel density, increased vessel permeability, enlargement of vessel diameter, and vascular reorganization in a non-uniform pattern [16–20]. Similarly, respiratory infection with herpes virus in mice induced endothelial cell proliferation and vessel thickening in the lung [21]. Previous studies have further suggested that these vascular changes were at least in part mediated by Angiopoietin/Tek receptor signaling. Overexpression of Angpt1 in pathogen-free mice induced the vascular remodeling similar to as in *Mycoplasma pulmonis* infected animals while blocking its effect by injection of soluble Tek receptor in infected animals inhibited the vascular responses to inflammation [22].

Prostatic inflammation is a common feature in aging men and is considered to be one of the major factors in the development and progression of BPH and its associated lower urinary tract symptoms (LUTS) as previous studies have demonstrated a strong association between the presence of prostatic inflammation and the increased incidence of BPH/LUTS [23–26]. In spite of this connection, the underlying mechanisms of how prostatic inflammation contributes to BPH/LUTS, has yet to be elucidated. There is increasing evidence suggesting that the vascular pathogenesis is a potential contributor to the etiology of BPH/LUTS. Studies in aging men have revealed that atherosclerotic diseases, such as coronary heart disease, hypertension, diabetes mellitus, are a risk factor for BPH/LUTS and are associated with the prevalence or symptom severity of BPH/LUTS [10–11, 27–32]. Subsequent studies on BPH have indicated that reduced prostatic blood flow and increased vascular resistance in the transition zone of the prostate were observed in patients with BPH/LUTS compared to control healthy group [10, 11]. It also appears that BPH/LUTS patients with vascular disorders had a greater reduction of prostatic blood flow and a greater severity of BPH symptoms than men without vascular disorders [10, 29]. Given that prostatic inflammation and vascular pathology are associated with BPH/LUTS and vascular response is essential during inflammation for tissue repair, the mechanisms underlying the vascular changes in response to inflammation in the prostate are postulated to contribute to the etiology of BPH/

LUTS. Therefore, it is tempting to investigate the effect of inflammation on vascular changes in the prostate.

In this study, the vascular development and its response to inflammation in the mouse prostate were described. We began the study by describing the vascular anatomy of the mouse prostate at the macroscopic level. We also evaluated the relationship of prostate vasculature with the epithelium, endothelial proliferation and mRNA expression of the major angiogenic factors in the developing and the mature adult mouse prostates. Finally exploiting our previously described mouse model of bacterial-induced prostatic inflammation [33], we characterized the vascular response to acute inflammation by measuring endothelial proliferation, vessel density and changes in the mRNA expression of the major angiogenic factors in the adult mouse prostate. The findings of this study are to serve as a fundamental resource for future research aimed at elucidating the role of vascular mechanisms in prostate development as well as the pathogenesis of inflammation associated prostatic diseases.

MATERIALS AND METHODS

Visualization of the Vascular System by Intra-cardiac Perfusion of India Ink

Adult C57BL6/J (Jackson Laboratory) or CD-1 WT (Charles River) male mice were used in these studies. To visualize the vascular anatomy of the mouse prostate, anesthetized mice were perfused with 25% India ink in sterile PBS through the left ventricle. India ink is commonly used in research for visualization of the blood vessels [34, 35]. After the ink is completely distributed to all vessels in the entire body, the urogenital tracts were removed immediately from the animals and were fixed in 10% neutral buffered formalin overnight at 4°C. The next day the tissues are rinsed in PBS and then incubated in PBS+1%KOH for two days at 4°C followed by serial steps with graded increasing concentration of glycerol in PBS +1% KOH starting at 25% to 50%, 75% and finally 100% for two days each with final storage in glycerol, all incubations done at 4°C. Note that as the concentration of glycerol goes up the concentration of the PBS/KOH goes down, starting with 1% KOH in PBS. The vasculature of the prostate was visualized under the dissecting light microscope and images were obtained using a digital SPOT camera.

Transurethral Instillation

Transurethral instillation was performed as previously described [33]. Briefly, eight to ten-week old CD-1 (Charles River) or C57BL6/J (Jackson Laboratory) WT male mice were anesthetized with isoflurane and a lubricated sterile polyethylene catheter was inserted into the mouse urethra. Uropathogenic *E. coli* 1677 (2×10^6CFU/ml) or sterile PBS in a volume of 200μl was instilled transurethrally into the adult male mice.

Animals were sacrificed 1, 2, 3, 5, and 7 days post-instillation. Naïve animals not undergoing instillation procedures were also sacrificed to control for vascular changes associated with catherization or transurethral instillation. In the study of the effect of prostatic inflammation on endothelial proliferation, animals were intraperitoneally injected with BrdU 2 hours prior to sacrifice and the prostate was collected from each animal for histology and immunohistochemistry. In the study of the effect of prostatic inflammation on gene expression of the angiogenic factors, the prostatic lobes were collected from each animal for RNA isolation. Four to seven mice per time point and per treatment were used. Ten animals without any treatment were sacrificed as naïve.

Vascular Development

CD-1 WT pregnant females and eight-week old male mice were purchased from Charles River. For study in quantitation of endothelial proliferation, animals were sacrificed at postnatal day 15 (n=6) and 8 week (n=6). Prostatic tissues were harvested and processed as described below for histology and immunohistochemistry. For study of angiogenic factor expressions, the male urogenital sinus (UGS) at embryonic day 16 (n=4), the prostate at postnatal day 5 (n=4) and the prostatic lobes at 8-week old animals (n=5) were collected for RNA isolation.

Immunohistochemical staining

Co-staining for Brdu and PECAM was used to assess the proliferation in endothelial cells. Tissue was removed from the animals and fixed in 4% PFA overnight at 4°C. PFA was replaced with 20% sucrose and incubated at 4°C for three days after which sucrose was replaced with OCT for 3 hours prior to embedding in fresh OCT. Samples were stored at −80°C until sectioned. Serially sections were cut at 10μm and slides stored at −80°C until staining. To begin staining tissue sections were washed in 0.01M PBS (pH 7.4) with 0.1% triton X100 (3× 5min). Incubate in 1N HCl for 10min on ice followed by 2N HCl for 10min at room temp and transfer to 37°C for another 20min. Immediately place in 0.1M borate buffer (pH 9) for 12min at room temp. Slides were then washed in PBS+0.1% TritonX100, three times 5min each at room temp. IHC blocking was with PBS (pH7.4)+0.1%TritonX100+Glycine (1M)+5% normal donkey serum for 1hr at room temp. Following blocking primary antibody in blocking solution was added, BrdU (Abcam 1893) at 1:50 dilution and PECAM (BD 550274) at 1:200 dilution. Primary antibodies were incubated at room temp overnight followed by three five min washes with PBS+0.1% TritonX100. Secondary staining was done with fluorescence antibodies from Invitrogen, (A21209, Alexa594 for PECAM, A11015, Alexa488 for BrdU) at 1:200 dilution in block buffer for 1hr at room temp. Wash three times as above for primary antibody. To stain nuclei add Hoechst 33258 at 4μg/ml in PBS for 10min at room temp. Wash three times, five min each in PBS, coverslip and image.

Co-staining for CDH1 and KDR was used to assess the relationship of the endothelial cells with the epithelial cells in the mouse UGS and prostate at different stages of development. Male urogenital sinus from E16.5, and prostates from P5, P20 and adult C57BL/6J mouse tissues were fixed in 4% paraformaldehyde, dehydrated in methanol, infiltrated with paraffin, and cut into 5-μm sections. After deparaffinization, hydration, and antigen unmasking in boiling 1mM Tris-EDTA buffer (pH 9), tissues were blocked for 1 hr in TBSTw containing 1% Blocking Reagent (Roche Diagnostics, Indianapolis, IN), 5% normal goat sera, and 1% bovine serum albumin fraction 5 (RGBTw). Tissues were incubated overnight at 4°C with primary antibodies diluted in RGBTw as follows: 1:250 mouse anti-CDH1 (61081, BD Transduction Laboratories, Franklin Lakes, NJ) and 1:600 rabbit anti-KDR (2479S, Cell Signaling Technology). Secondary antibodies were diluted as follows: 1:250 Dylight 488-conjugated anti-mouse IgG (115-487-003, Jackson Immunoresearch, West Grove, PA), 1:250 Alexa Fluor 594 Goat Anti-Rabbit IgG (A11012, Life Technologies, Grand Island, NY). Immunofluorecent labeled tissues were counterstained with 4′,6-diamidino-2-phenylindole, dilactate, and mounted in anti-fade media (phosphate-buffered saline containing 80% glycerol and 0.2% n-propyl gallate).

Mean Blood Vessel Density (MVD)

Eight to twelve-week old C57BL6/J WT male mice (Jackson Laboratory) were instilled transurethrally with uropathogenic *E. coli* or sterile saline as described above. Prostatic tissues at day 3 (n=4 saline, n=3 *E. coli)* and 7 (n=4 saline, n=4 *E. coli)* post-instillation were harvested, fixed in 10% formalin, embedded in paraffin and serially sectioned at 6μm.

Standard H&E staining were performed for histology. The severity of inflammation was graded based on our previous established grading system [33]. The identification of blood vessels in the H&E images was consulted with a pathologist. The number of blood vessels in the stromal area per 10X field were counted and used to determine MVD for the DLP. The data are presented as the mean ± SEM.

Endothelial Proliferation

Immunohistochemical staining for BrdU and PECAM were performed on frozen sections as described above. 20X field images were obtained using an Olympus fluorescent microscope and a digital SPOT camera. Double positive BrdU/PECAM (+/+) cells representing endothelial proliferation were counted. For developmental experiments comparisons were made between animals at P15 and 8-week old. Comparisons between saline and 3, 5, 7-day *E. coli* post-instillation were used to assess proliferation during inflammation. In addition, H&E staining for histology was performed to confirm prostatic inflammation in the *E. coli* infected animals. The data are presented as the mean ± SEM.

RNA isolation and cDNA

UGS tissues and prostatic lobes from animals were collected in 1.6ml microcentrifuge tubes and snap frozen in liquid nitrogen immediately. RNA from the tissues was extracted using RNeasy Micro Kit (Qiagen, Inc.) and following the manufacture's protocol and RNA yield was measured and purity determined by 260/280nm ratio on a Nanodrop 1000 spectrophotometer (Thermo Scientific Inc.). RNA was converted to cDNA by reverse transcription as previously described [33].

Semi-Quantitative Real-Time PCR

Semi-quantitative RT-PCR was performed with cDNA samples to quantitate gene expression levels of the angiogenic factors. The forward and reverse primers of each angiogenic factor Pecam, Pdgfa, Tie1, Tek, Angpt1, Angpt2, Angpt4, Fgf2, Vegfa, Vegfb, Vegfc, and *Figf* were designed using the NCBI mouse nucleotide database, the mouse genomic BLAST database and the Primer-3 program. The sequences of the primers used are shown in Table I. RT-PCR cycle reactions were detected with SYBR green (Roche) and run on a BioRad Real-Time CFX with run conditions of 95°C for 10 minutes, followed by 50 cycles of 95°C for 15 seconds and 60°C for 1 minute. Gene expression levels were normalized to the housekeeping gene *Gapdh*.

Statistical Analysis

Gene expression between different time periods was compared using ANOVA (analysis of variance), followed by a Fisher's LSD (Least Significant Difference) test for pair-wise comparisons of different time periods. Prior to ANOVA, Levene's test was used to verify the homoscedasticity assumption and a non-parametric procedure was used for non-conforming data. All analysis was conducted using SAS 9.2 (SAS Institute, Cary NC) software. A p-value < 0.05 was considered statistically significant in two-tailed statistical tests.

To explore the relationship between mean vessel density and inflammation score for different prostatic lobes, Spearman's rank correlation coefficient (ρ) was calculated together with its test statistic. Commonly the strength of the correlation ranges from -1 to 1, with values closer to 1 indicating very strong correlation and to 0 representing very weak correlation. The sign (+ or −) of the correlation coefficient defines the direction of the relationship. Further, a comparison was performed on the inflammation score between WT and *E. coli* for different prostatic lobes on day 3 and 7 using a two-sample t-test. All analysis

was conducted using SAS 9.2 (SAS Institute, Cary NC) software. A p-value < 0.05 was considered statistically significant in two-tailed statistical tests.

RESULTS

Vascular Anatomy of the Adult Mouse Prostate

We investigated the vascular anatomy of the adult mouse prostate vasculature by intra-cardiac injection of India ink and light microscopy (Figure 1 A and B). The India ink angiograms revealed one main artery on each side of the ventral aspect of the bladder supplying the prostate/seminal vesicle complex. This artery branches into three vessels near the neck of the bladder to supply the bladder, prostate, seminal vesicle and the urethra. The central branch bifurcates - giving off one vessel that runs along the anterior prostate to supply the anterior prostatic ducts and parts of the adjacent seminal vesicle and another vessel that directly supplies the anterior prostate. The dorsal branch supplies the dorsolateral prostate while the ventral branch supplies the ventral surface of the bladder and the ventral prostate. Vessels supplying the ventral and dorsolateral prostate lobes enter near the junction of the main prostate ducts with the urethra and arborize as they extend distally (Figure 1C and D). Schematic illustrations of the vascular anatomy of the adult male mouse urogenital tract are shown in Figure 1E and F.

Architecture of vascular development

To visualize the relationship between microvessels and prostate ducts during their initial outgrowth (E16.5), branching morphogenesis (P5), glandularization (P20), and upon maturation (P50), we conducted double immunofluorescent staining for vascular endothelial growth factor receptor 2 (VEGFR2 also known as KDR, marks endothelium) and cadherin 1 (CDH1, marks prostatic epithelium). We observed a distinct vascular network in the stroma along the entire cranial-caudal axis of the urethra of the male UGS at E16.5 (Figure 2A). This network was also detected in the stroma of the seminal vesicle and ejaculatory duct epithelium, similar to the observations made by Abler et al., 2011 [36]. Importantly, a discernible vascular network circumscribed nascent ducts from the very beginning of their development, suggesting a coordinated mechanism of pattern formation (Figure 2A). A similar spatial relationship was observed at P5, when microvessels enveloped newly formed prostatic branch tips (Figure 2B). Vessels were oriented along the proximodistal duct axis at P20 (Figure 2C) and P50 (Figure 2D), again suggesting coordination in patterning of prostatic ducts and the prostatic vascular supply.

Angiogenic Factor Expression in Mouse Prostate Development

We analyzed mRNA expression pattern of angiogenic factors in the male E16 UGS, P5 prostate and the individual lobes of the adult prostate (Figure 3). Expression of Pecam1, Tie1, Tek, Angpt1, Angpt2, Fgf2, Vegfc, and Figf was higher at E16 than at the adult stage. A subset of these genes (*Tie1*, *Tek*, *Angpt1*, *Fgf2*, *Vegfc*, and *Figf)* as well as *Vegfa*, were expressed more abundantly at P5 as well. Several genes, including *Angpt2*, *Angpt4* and *Vegfb*, did not exhibit increased expression at either E16 or P5 and actually seemed to be expressed more abundantly in the adult. In contrast, *Pdgfa* showed no significant differences in expression at any of the time points examined. All of the angiogenic factors examined have been shown to have important functions associated with angiogenesis. However, their angiogenic effects are highly dependent on the presence of each other and the interaction with specific receptors [37, 38]. Further, many of these angiogenic factors have multiple isoforms with variable potency and activity [37, 38]. It is therefore difficult to directly correlate the temporal patterns of mRNA expression for any factor with a specific angiogenic process in either the developing or adult prostate. However, our finding that a majority of angiogenic factors are expressed more abundantly in the perinatal period is

clearly consistent with generally robust angiogenic activity required for vascularization of the growing prostate.

Vascular Response to Acute Inflammation in the Mouse Prostate

To assess the response of vasculature in bacterial-induced injury and inflammation we measured the mean blood vessel density, endothelial cell proliferation and the expression profiles of angiogenic genes in the DLP following bacterial infection. The DLP was selected for analysis since our previous work has shown that the DLP exhibits the most consistent and robust inflammatory response to bacterial inoculation [33]. Analysis of H&E stained sections showed a significant increase of inflammatory degree and mean blood vessel density in the stromal area of the DLP of the *E. coli* infected mice at day 3 and 7 post-instillation (Figure 4A and B). Correlation analysis revealed a strong positive relationship between the severity of inflammation and the mean blood vessel density (Figure 4C and D). To determine whether increased mean vessel density is associated with an increase in endothelial proliferation, mice were injected IP with BrdU 2 hours before sacrifice. Proliferating endothelial cells were identified by co-immunostaining for BrdU and the endothelial marker (PECAM). The number of double positive PECAM/BrdU (+/+) cells was sixteen-fold higher on day 3 post-infection as compared to saline control. Endothelial proliferation returned to baseline by day 5 post-infection (Figure 5A–D, G). There was no difference in endothelial BrdU labeling index between naïve and saline controls (data not shown), demonstrating that the instillation procedure itself had no effect on endothelial proliferation. To ascertain the relative magnitude of the proliferative response induced by inflammation of the adult prostate, we compared the endothelial labeling index in adult and P15 mice. P15 is a period of robust ductal morphogenesis and growth of the prostate ductal network is at its peak. This revealed that endothelial proliferation was six-fold higher at P15 than in the adult (Figure 5E–F, H). These data show that there is a rapid vascular response to bacterial-induced inflammation that is characterized by a very robust increase in endothelial proliferation.

Angiogenic Factor Expression in the Bacterial-Inflamed Prostate

We analyzed mRNA expression pattern of angiogenic factors in the DLP (Figure 6) of the adult mice at day 1, 2, 3, 5, and 7 post-instillation. Expression of Pecam, Pdgfa, Tie1, Tek, Angpt1, Angpt2, Angpt4, Fgf2, Vegfb, Vegfc, and *Figf* decreased significantly in the first three days following bacterial infection. By day 5 and 7 post-infection, expression of most of these genes (Pdgfa, Tie1, Tek, Angpt1, Angpt2, Angpt4, Fgf2, Vegfb, and *Vegfc*) returned to baseline while *Pecam* and *Figf* exhibited a rebound expression significantly higher than baseline. Expression of *Vegfa* showed no significant changes at any time point.

DISCUSSION

We used intra-cardiac injection of India ink to visualize the mouse prostatic vasculature. Injection into the beating heart allowed the ink to distribute through the arterial system. We observed a single main artery on the ventral aspect of each side of the bladder running laterally onto the side of the prostatic urethra and trifurcating near the bladder neck. The ventral branch supplies the bladder and the ventral prostate; the central branch supplies the seminal vesicle and the anterior prostate; the dorsal branch supplies the dorsolateral prostate.

Immunonstaining for VEGFR2 in the UGS demonstrated an abundant microvessel network circumscribing the newly formed prostatic bud. This network enveloped the elongating ducts and duct tips postnatally and generated the microvascular network of the adult prostate. These observations complement a detailed electron-microscopy study of the microvascular network in the adult rat previously published by Buttyan and colleagues [12].

Formation of this vascular network during prostate development was accompanied by robust expression of a variety of angiogenic factors, including Pecam1, Tie1, Tek, Angpt1, Angpt2, Fgf2, Vegfa, Vegfc, and Figf. The association of angiogenic factor expression with development of the vascular network is compelling, however, we cannot at this time ascribe a specific role to any single or group of factors in the process of endothelial proliferation and vascular remodeling in the prostate.

We observed a dramatic increase in endothelial proliferation in response to bacterial-induced prostatic inflammation. Endothelial proliferation was increased 16-fold 3 days after bacterial inoculation and decreased to baseline 5 days post-inoculation. Vascular density was also increased. The magnitude of the vascular response to bacterial-induced inflammation was assessed by comparing it to the angiogenic activity in the adolescent (P15) and the normal adult prostate. We selected the P15 for comparison because P15 is a period of robust ductal morphogenesis [39]. These studies revealed that endothelial proliferation was 6-fold higher at P15 than in the adult, but the relative increase in proliferation was even higher in the inflamed prostate. The increase in endothelial proliferation 3 days post-infection occurs concomitant with a marked increase in epithelial proliferation as previously reported [33, 40].

Angiogenesis is a critical step during inflammation in response to tissue injury and is tightly mediated by a variety of angiogenic factors. The resulting new vessels are essential to provide oxygen in wounded area and facilitate tissue regeneration. Previous studies have shown that airway inflammation induced by *Mycoplasma pulmonis* infection in C3H/HeN mice increased angiogenesis as evidenced by increased endothelial cell proliferation beginning as early as 1 day following infection [16]. The proliferative index of endothelial cells peaked at 5 days, and sharply declined at day 9 post-infection but remained higher than uninfected control. This angiogenic response to airway inflammation was accompanied by numerous vascular modeling including enlargement of existing vessels, endothelial cell enlargement and increased vessel density.

We found mRNA expression of a majority of angiogenic factors examined to be decreased in the prostate after bacterial infection. This finding stands at odds with the robust endothelial proliferation that accompanies the inflammatory response. It is, to our knowledge, without precedent in the literature. One possible explanation is that inflammation/injury induces the release of previously synthesized angiogenic factors. An alternative explanation is that endothelial proliferation during bacterial-induced inflammation may not be mediated by the angiogenic factors examined in this study but instead by other factors produced following bacterial-infection. We have previously shown that IL-1 is highly expressed in prostatic inflammation and is required for the epithelial hyperplasia that occurs in response to bacterial-induced inflammation [40]. IL-1 has been demonstrated to be pro-angiogenic and might contribute to the angiogenic response observed. Previous studies have suggested that IL-1 can elicit production of both classical pro-angiogenic factors and inflammatory cytokines such as IL-8, TNFα, HGF, TGFβ, and COX2 that possess angiogenic activity [40, 43–51].

Despite the extensive focus in studying the pathogenesis of BPH, the role of angiogenesis and the angiogenic factors in BPH is poorly studied. Previous studies have showed that microvascularity was increased in BPH [9]. However, subsequent studies to characterize the pro-angiogenic factor expression in BPH tissues are controversial. Studies by Jackson et al have shown 100% cases of BPH were stained positive for VEGFA [52]. Stefanou and colleagues have reported that VEGFA were expressed in 81.25% of BPH samples examined [53]. In contrast, another studies have found that 83% of BPH cases were negative for VEGFA [54]. Thus, it is unclear whether the classical pro-angiogenic factors are important

in regulating angiogenesis in BPH due to these inconsistent findings. Intriguingly, previous studies have shown that inflammatory factors including IL-1, IL-8, TGFβ were capable to mediate angiogenesis in addition to their typical inflammatory functions and more importantly, these factors were highly expressed in some cases of BPH tissues with inflammation [40, 43–59]. Given that angiogenesis is a typical vascular response to inflammation and prostatic inflammation is a common feature in BPH, it is tempting to speculate that prostatic inflammation in BPH induces vascular remodeling through the angiogenic effects of the inflammatory cytokines. The findings in our studies support this concept, leading to a hypothesis that angiogenesis in response to prostatic inflammation may be mediated by inflammatory cytokines rather than the classical angiogenic factors. This suggests a mechanism that may explain the inconsistent findings of the correlation between angiogenesis and classical angiogenic factor expression in BPH and provide a new perspective for a possible role of inflammation-induced vascular remodeling and angiogenesis in the pathogenesis of BPH.

CONCLUSIONS

The developing prostate and the inflamed adult prostate both exhibit robust endothelial proliferation. However, the endothelial proliferation associated with inflammation is characterized by a decrease in pro-angiogenic factor mRNA expression suggesting that it is not a recapitulation of normal vascular development but a process initiated and regulated by a different set of regulatory factors.

Acknowledgments

This work was supported by NIH R01DK0757 and T32 ES007015 from the National Institute of Environmental Health Sciences (NIEHS), NIH. Its contents are solely the responsibility of the authors and do not necessarily represent the official views of the NIEHS, NIH. The authors also greatly appreciate the help from M. Shahriar Salamat, MD, PhD with his knowledge in pathology.

Grant sponsor: NIH; Grant number: 1R01DK0757; Grant sponsor: National Institute of Environmental Health Sciences; Grant number: T32 ES007015

ABBREVIATIONS

Angpt	angiopoietins
AP	anterior prostate
BPH	benign prostatic hyperplasia
BrdU	5-bromo-2-deoxyuridine
DLP	dorsal-lateral prostate
Fgf	fibroblast growth factor
H&E	hematoxylin and eosin
IHC	immunohistochemistry
IP	intraperitoneal
LUTS	lower urinary tract symptoms
MVD	mean vessel density
Pdgf	platelet-derived growth factor
Pecam	platelet endothelial cell adhesion molecule

RNA	ribonucleic acid
RT-PCR	real-time polymerase chain reaction
Tek	endothelial tyrosine kinase
Tie1	tyrosine kinase with immunoglobulin-like and EGF-like domains 1
UGS	urogenital sinus
Vegf	vascular endothelial growth factor
VP	ventral prostate

REFERENCE

1. Lekas E, Johansoon M, Widmark A, Bergh A, Damber JE. Decrement of blood flow precedes the involution of the ventral prostate in the rat after castration. Urol Res. 1997; 25(5):309–14. [PubMed: 9373910]
2. Shabisgh A, Tanji N, D'Agati V, Burchardt M, Rubin M, Goluboff ET, Heitjan D, Kiss A, Buttyan R. Early effects of castration on the vascular system of the rat ventral prostate gland. Endocrinology. 1999; 140(4):1920–6. [PubMed: 10098532]
3. Shabsigh A, Chang DT, Heitjan DF, Kiss A, Olsson CA, Puchner PJ, Buttyan R. Rapid reduction in blood flow to the rat ventral prostate gland after castration: preliminary evidence that androgens influence prostate size by regulating blood flow to the prostate gland and prostatic endothelial cell survival. Prostate. 1998; 36(3):201–6. [PubMed: 9687993]
4. Franck-Lissbrant I, Häggström S, Damber JE, Bergh A. Testosterone stimulates angiogenesis and vascular regrowth in the ventral prostate in castrated adult rats. Endocrinology. 1998; 139(2):451–6. [PubMed: 9449610]
5. Lekas E, Engstrand C, Bergh A, Damber JE. Transient ischemia induces apoptosis in the ventral prostate of the rat. Urol Res. 1999; 27(3):174–9. [PubMed: 10422818]
6. Kozlowski R, Kershen RT, Siroky MB, Krane RJ, Azadzoi KM. Chronic ischemia alters prostate structure and reactivity in rabbits. J Urol. 2001; 165(3):1019–26. [PubMed: 11176533]
7. Shibata Y, Kashiwagi B, Arai S, Fukabori Y, Suzuki K, Honma S, Yamanaka H. Direct regulation of prostate blood flow by vascular endothelial growth factor and its participation in the androgenic regulation of prostate blood flow in vivo. Endocrinology. 2004; 145(10):4507–12. [PubMed: 15231711]
8. Bigler SA, Deering RE, Brawer MK. Comparison of microscopic vascularity in benign and malignant prostate tissue. Hum Pathol. 1993; 24(2):220–6. [PubMed: 8432518]
9. Deering RE, Bigler SA, Brown M, Brawer MK. Microvascularity in benign prostatic hyperplasia. Prostate. 1995; 26(3):111–5. [PubMed: 7534916]
10. Berger AP, Deibl M, Leonhartsberger N, Bektic J, Horninger W, Fritsche G, Steiner H, Pelzer AE, Bartsch G, Frauscher F. Vascular damage as a risk factor for benign prostatic hyperplasia and erectile dysfunction. BJU Int. 2005; 96(7):1073–8. [PubMed: 16225531]
11. Berger AP, Horninger W, Bektic J, Pelzer A, Spranger R, Bartsch G, Frauscher F. *V*ascular resistance in the prostate evaluated by colour Doppler ultrasonography: is benign prostatic hyperplasia a vascular disease? BJU Int. 2006; 98(3):587–90. [PubMed: 16796699]
12. Shabsigh A, Tanji N, D'Agati V, Burchardt T, Burchardt M, Hayek O, Shabisgh R, Buttyan R. Vascular anatomy of the rat ventral prostate. Anat Rec. 1999; 256(4):403–11. [PubMed: 10589026]
13. Li J, Chen J, Kirsner R. Pathophysiology of acute wound healing. Clin Dermatol. 2007; 25(1):9–18. [PubMed: 17276196]
14. Li J, Zhang YP, Kirsner RS. Angiogenesis in wound repair: angiogenic growth factors and the extracellular matrix. Microsc Res Tech. 2003; 60(1):107–14. [PubMed: 12500267]
15. Diegelmann RF, Evans MC. Wound healing: an overview of acute, fibrotic and delayed healing. Front Biosci. 2004; 9:283–9. [PubMed: 14766366]

16. Ezaki T, Baluk P, Thurston G, La Barbara A, Woo C, McDonald DM. Time course of endothelial cell proliferation and microvascular remodeling in chronic inflammation. Am J Pathol. 2001; 158(6):2043–55. [PubMed: 11395382]

17. Dahlqvist K, Umemoto EY, Brokaw JJ, Dupuis M, McDonald DM. Tissue macrophages associated with angiogenesis in chronic airway inflammation in rats. Am J Respir Cell Mol Biol. 1999; 20(2): 237–47. [PubMed: 9922214]

18. Aurora AB, Baluk P, Zhang D, Sidhu SS, Dolganov GM, Basbaum C, McDonald DM, Killeen N. Immune complex-dependent remodeling of the airway vasculature in response to a chronic bacterial infection. J Immunol. 2005; 175(10):6319–26. [PubMed: 16272283]

19. Baluk P, Yao LC, Feng J, Romano T, Jung SS, Schreiter JL, Yan L, Shealy DJ, McDonald DM. TNF-alpha drives remodeling of blood vessels and lymphatics in sustained airway inflammation in mice. J Clin Invest. 2009; 119(10):2954–64. [PubMed: 19759514]

20. Kwan ML, Gómez AD, Baluk P, Hashizume H, McDonald DM. Airway vasculature after mycoplasma infection: chronic leakiness and selective hypersensitivity to substance P. Am J Physiol Lung Cell Mol Physiol. 2001; 280(2):L286–97. [PubMed: 11159008]

21. Calabrese F, Kipar A, Lunardi F, Balestro E, Perissinotto E, Rossi E, Nannini N, Marulli G, Stewart JP, Rea F. Herpes virus infection is associated with vascular remodeling and pulmonary hypertension in idiopathic pulmonary fibrosis. PLoS One. 2013; 8(2):e55715. [PubMed: 23468849]

22. Fuxe J, Lashnits E, O'Brien S, Baluk P, Tabruyn SP, Kuhnert F, Kuo C, Thurston G, McDonald DM. Angiopoietin/Tie2 signaling transforms capillaries into venules primed for leukocyte trafficking in airway inflammation. Am J Pathol. 2010; 176(4):2009–18. [PubMed: 20133818]

23. Robert G, Descazeaud A, Nicolaïew N, Terry S, Sirab N, Vacherot F, Maillé P, Allory Y, de la Taille A. Inflammation in benign prostatic hyperplasia: a 282 patients' immunohistochemical analysis. Prostate. 2009; 69(16):1774–80. [PubMed: 19670242]

24. Kramer G, Steiner GE, Handisurya A, Stix U, Haitel A, Knerer B, Gessl A, Lee C, Marberger M. Increased expression of lymphocyte-derived cytokines in benign hyperplastic prostate tissue, identification of the producing cell types, and effect of differentially expressed cytokines on stromal cell proliferation. Prostate. 2002; 52(1):43–58. [PubMed: 11992619]

25. Steiner GE, Stix U, Handisurya A, Willheim M, Haitel A, Reithmayr F, Paikl D, Ecker RC, Hrachowitz K, Kramer G, Lee C, Marberger M. Cytokine expression pattern in benign prostatic hyperplasia infiltrating T cells and impact of lymphocytic infiltration on cytokine mRNA profile in prostatic tissue. Lab Invest. 2003; 83(8):1131–46. [PubMed: 12920242]

26. Theyer G, Kramer G, Assmann I, Sherwood E, Preinfalk W, Marberger M, Zechner O, Steiner GE. Phenotypic characterization of infilitrating leukocytes in benign prostatic hyperplasia. Lab Invest. 1992; 66(1):96–107. [PubMed: 1370561]

27. Berger AP, Deibl M, Halpern EJ, Lechleitner M, Bektic J, Horninger W, Fritsche G, Steiner H, Pelzer A, Bartsch G, Frauscher F. Vascular damage induced by type 2 diabetes mellitus as a risk factor for benign prostatic hyperplasia. Diabetologia. 2005; 48(4):784–9. [PubMed: 15756540]

28. Berger AP, Bartsch G, Deibl M, Alber H, Pachinger O, Fritsche G, Rantner B, Fraedrich G, Pallwein L, Aigner F, Horninger W, Frauscher F. Atherosclerosis as a risk factor for benign prostatic hyperplasia. BJU Int. 2006; 98(5):1038–42. [PubMed: 16879445]

29. Michel MC, Mehlburger L, Schumacher H, Bressel HU, Goepel M. Effect of diabetes on lower urinary tract symptoms in patients with benign prostatic hyperplasia. J Urol. 2000; 163(6):1725–9. [PubMed: 10799169]

30. Bourke JB, Griffin JP. Hypertension, diabetes mellitus, and blood groups in benign prostatic hypertrophy. Br J Urol. 1966; 38(1):18–23. [PubMed: 4143704]

31. Weisman KM, Larijani GE, Goldstein MR, Goldberg ME. Relationship between benign prostatic hyperplasia and history of coronary artery disease in elderly men. Pharmacotherapy. 2000; 20(4): 383–6. [PubMed: 10772367]

32. Meigs JB, Mohr B, Barry MJ, Collins MM, McKinlay JB. Risk factors for clinical benign prostatic hyperplasia in a community-based population of healthy aging men. J Clin Epidemiol. 2001; 54(9):935–44. [PubMed: 11520654]

33. Boehm BJ, Colopy SA, Jerde TJ, Loftus CJ, Bushman W. Acute bacterial inflammation of the mouse prostate. Prostate. 2012; 72(3):307–17. [PubMed: 21681776]
34. Nagy A. Visualizing fetal mouse vasculature by India ink injection. Cold Spring Harb Protoc. 2010; 2010(2):pdb prot5371. [PubMed: 20150134]
35. Hasan MR, Herz J, Hermann DM, Doeppner TR. Intravascular perfusion of carbon black ink allows reliable visualization of cerebral vessels. J Vis Exp. 2013; (71)
36. Abler LL, Keil KP, Mehta V, Joshi PS, Schmit CT, Vezina CM. A high-resolution molecular atlas of the fetal mouse lower urogenital tract. Dev Dyn. 2011; 240(10):2364–77. [PubMed: 21905163]
37. Ferrara N. Role of vascular endothelial growth factor in regulation of physiological angiogenesis. Am J Physiol Cell Physiol. 2001; 280(6):C1358–66. [PubMed: 11350730]
38. Bouïs D, Kusumanto Y, Meijer C, Mulder NH, Hospers GA. A review on pro- and anti-angiogenic factors as targets of clinical intervention. Pharmacological Research. 2006; 53:89–103. [PubMed: 16321545]
39. Sugimura Y, Cunha GR, Donjacour AA. Morphogenesis of ductal networks in the mouse prostate. Biol Reprod. 1986; 34(5):961–71. [PubMed: 3730488]
40. Jerde TJ, Bushman W. IL-1 induces IGF-dependent epithelial proliferation in prostate development and reactive hyperplasia. Sci Signal. 2009; 2(86):ra49. [PubMed: 19724062]
41. Baluk P, Tammela T, Ator E, Lyubynska N, Achen MG, Hicklin DJ, Jeltsch M, Petrova TV, Pytowski B, Stacker SA, Ylä-Herttuala S, Jackson DG, Alitalo K, McDonald DM. Pathogenesis of persistent lymphatic vessel hyperplasia in chronic airway inflammation. J Clin Invest. 2005; 115(2):247–57. [PubMed: 15668734]
42. Tabruyn SP, Colton K, Morisada T, Fuxe J, Wiegand SJ, Thurston G, Coyle AJ, Connor J, McDonald DM. Angiopoietin-2-driven vascular remodeling in airway inflammation. Am J Pathol. 2010; 177(6):3233–43. [PubMed: 20952594]
43. Doll JA, Reiher FK, Crawford SE, Pins MR, Campbell SC, Bouck NP. Thrombospondin-1, vascular endothelial growth factor and fibroblast growth factor-2 are key functional regulators of angiogenesis in the prostate. Prostate. 2001; 49(4):293–305. [PubMed: 11746276]
44. Voronov E, Shouval DS, Krelin Y, Cagnano E, Benharroch D, Iwakura Y, Dinarello CA, Apte RN. IL-1 is required for tumor invasiveness and angiogenesis. Proc Natl Acad Sci USA. 2003; 100(5): 2645–50. [PubMed: 12598651]
45. Bar D, Apte RN, Voronov E, Dinarello CA, Cohen S. A continuous delivery system of IL-1 receptor antagonist reduces angiogenesis and inhibits tumor development. FASEB J. 2004; 18(1): 161–3. [PubMed: 14597552]
46. Saijo Y, Tanaka M, Miki M, Usui K, Suzuki T, Maemondo M, Hong X, Tazawa R, Kikuchi T, Matsushima K, Nukiwa T. Proinflammatory cytokine IL-1 beta promotes tumor growth of Lewis lung carcinoma by induction of angiogenic factors: in vivo analysis of tumor-stromal interaction. J Immunol. 2002; 169(1):469–75. [PubMed: 12077278]
47. Carmi Y, Voronov E, Dotan S, Lahat N, Rahat MA, Fogel M, Huszar M, White MR, Dinarello CA, Apte RN. The role of macrophage-derived IL-1 in induction and maintenance of angiogenesis. J Immunol. 2009; 183:4705–14. &. [PubMed: 19752225]
48. Bussolino F, Di Renzo MF, Ziche M, Bocchietto E, Olivero M, Naldini L, Gaudino G, Tamagnone L, Coffer A, Comoglio PM. Hepatocyte growth factor is a potent angiogenic factor which stimulates endothelial cell motility and growth. J Cell Biol. 1992; 119(3):629–41. [PubMed: 1383237]
49. Kuwano T, Nakao S, Yamamoto H, Tsuneyoshi M, Yamamoto T, Kuwano M, Ono M. Cyclooxygenase 2 is a key enzyme for inflammatory cytokine-induced angiogenesis. FASEB J. 2004; 18(2):300–10. [PubMed: 14769824]
50. Koch AE, Polverini PJ, Kunkel SL, Harlow LA, DiPietro LA, Elner VM, Elner SG, Strieter RM. Interleukin-8 as a marcophage-derived mediator of angiogenesis. Science. 1992; 258(5089):1798–1801. [PubMed: 1281554]
51. Torisu H, Ono M, Kiryu H, Furue M, Ohmoto Y, Nakayama J, Nishioka Y, Sone S, Kuwano M. Macrophage infiltration correlates with tumor stage and angiogenesis in human malignant melanoma- possible involvement of TNFalpha and IL-1alpha. Int J Cancer. 2000; 85(2):182–8. [PubMed: 10629075]

52. Jackson MW, Bentel JM, Tilley WD. Vascular endothelial growth factor (VEGF) expression in prostate cancer and benign prostatic hyperplasia. J Urol. 1997; 157(6):2323–8. [PubMed: 9146664]

53. Stefanou D, Batistatou A, Kamina S, Arkoumani E, Papachristou J, Agnantis NJ. Expression of vascular endothelial growth factor (VEGF) and association with microvessel density in benign prostatic hyperplasia and prostate cancer. In Vivo. 2004; 18(2):155–60. [PubMed: 15113042]

54. Gyftopoulos K, Vourda K, Sakellaropoulos G, Perimenis P, Athanasopoulos A, Papadaki E. The angiogenic switch for vascular endothelial growth factor-A and cyclooxygenase-2 in prostate carcinoma: correlation with microvessel density, androgen receptor content and Gleason grade. Urol Int. 2011; 87(4):464–9. [PubMed: 21912077]

55. Mori H, Maki M, Oishi K, Jaye M, Igarashi K, Yoshida O, Hatanaka M. Increased expression of genes for basic fibroblast growth factor and transforming growth factor type beta 2 in human benign prostatic hyperplasia. Prostate. 1990; 16(1):71–80. [PubMed: 1689483]

56. Schauer IG, Ressier SJ, Tuxhorn JA, Dang TD, Rowley DR. Elevated epithelial expression of interleukin-8 correlates with myofibroblast reactive stroma in benign prostatic hyperplasia. Urology. 2008; 72(1):205–13. [PubMed: 18314176]

57. König JE, Senge T, Allhoff EP, König W. Analysis of the inflammatory network in benign prostatic hyperplasia. Prostate. 2004; 58(2):121–9. [PubMed: 14716737]

58. Djonov V, Ball RK, Graf S, Mottaz AE, Arnold AM, Flanders K, Studer UE, Merz VW. Transforming growth factor-beta 3 is expressed in nondividing basal epithelial cells in normal human prostate and benign prostatic hyperplasia, and is no longer detectable in prostate carcinoma. Prostate. 1997; 31(2):103–9. [PubMed: 9140123]

59. Timme TL, Yang G, Truong LD, Kadmon D, Park SH, Thompson TC. Transforming growth factor-beta localization during mouse prostate morphogenesis and in prostatic growth abnormalities. World J Urol. 1995; 13(6):324–8. [PubMed: 9116750]

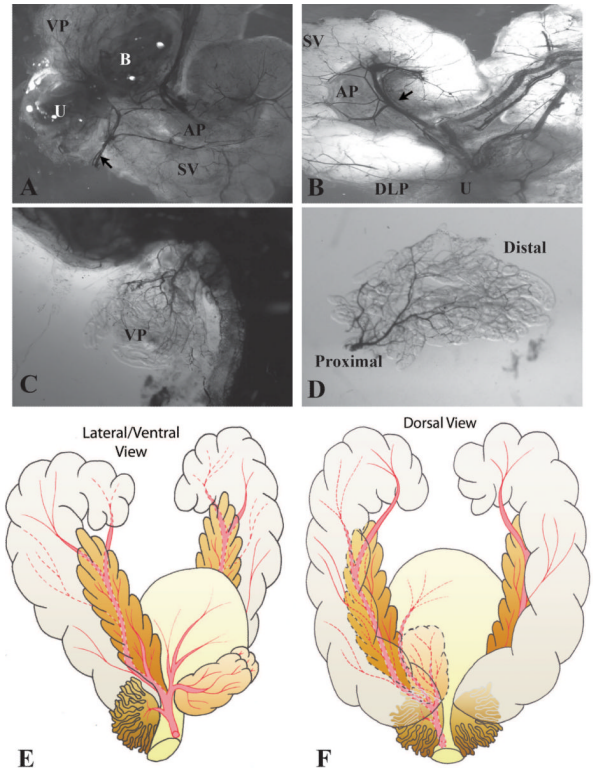

Figure 1.

Visualization of the prostatic vascular anatomy by intracardiac perfusion of India ink. **A.** Low magnification brightfield image of the ventral and lateral side of adult male mouse urogenital tract. The blood vessels were filled with black India ink. Black arrow indicates the main artery supplying the male urogenital tract. Note that left lobe of the ventral prostate was removed to visualize the vessels near the neck of the bladder. **B.** Low magnification brightfield image of the dorsal side of adult mouse male urogenital tract. Black arrow indicates the main artery supplying the seminal vesicle and anterior prostate. **C–D.** Images of ventral prostate showing that the vessels supplying the lobe enter close to the urethra and arborize distally. U Urethra. VP Ventral prostate. DLP Dorsalateral prostate. AP Anterior prostate. SV Seminal vesicle. B Bladder. **E–F.** Schematic illustrations of the vascular anatomy of the adult male mouse urogenital tract. **E.** A lateral and ventral view. **F.** A dorsal view. The main artery on the ventral aspect of the bladder runs laterally onto each side of the male urethra and branches into three vessels near the neck of the bladder: the ventral branch supplies the bladder and the ventral prostate; the central branch supplies the seminal vesicle and the anterior prostate; the dorsal branch supplies the dorsolateral prostate.

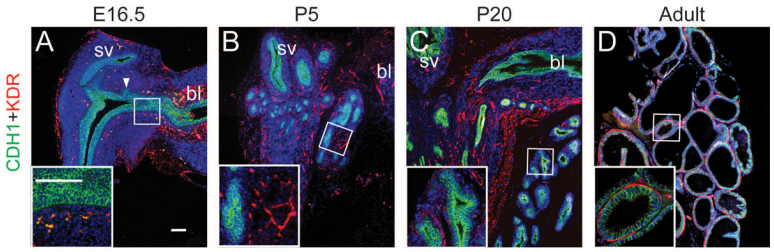

Figure 2.

Immunostaining for CDH1 (Green), KDR (Red) and DAPI (Blue) in the E16.5 UGS **(A)**, P5 ventral prostate **(B)**, P20 ventral prostate **(C)**, adult ventral prostate **(D)**. bl: bladder, sv: seminal vesicle. In panel A, arrowheads indicate prostatic bud. Scale bars in panel A and inset correspond to 100μm. Note that there is abundant auto-fluorescence of the red blood cells shown as yellow in the E16.5 UGS.

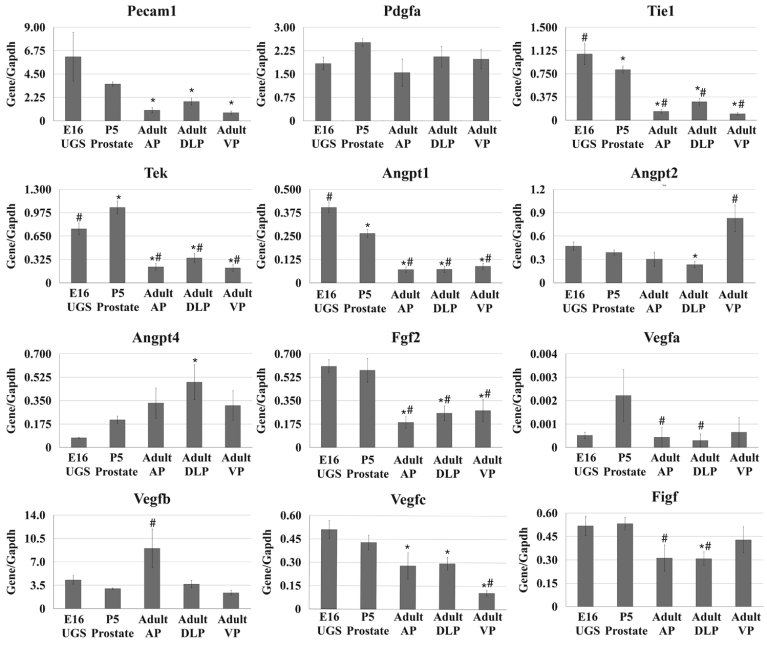

Figure 3.

qRT-PCR analysis for the angiogenic factors in the E16 male UGS, P5 prostate, and the AP, DLP, VP of the adult. The data are presented as the mean ± SEM. * indicates a p-value < 0.05 compared to E16 UGS by two-sample t-test. # indicates a p-value < 0.05 compared to P5 prostate by two-sample t-test. UGS Urogenital sinus. AP Anterior prostate. DLP Dorsolateral prostate. VP Ventral prostate.

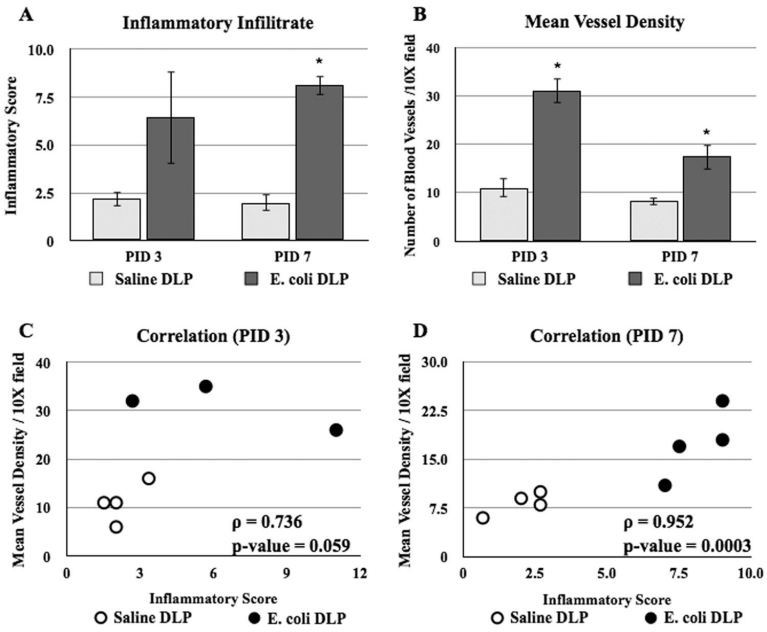

Figure 4.

Vascular response to bacterial-induced acute inflammation. **A.** Comparisons of the inflammatory infiltrate in the DLP of the saline and *E. coli* infected adult male mice at day 3 and 7 post-instillation (n=4 each time point). **B.** Comparisons of the mean blood vessel density in the DLP of the saline and *E. coli* infected adult male mice at day 3 and 7 post-instillation (n=4 each time point). The data are presented as the mean ± SEM. * indicates p-value < 0.05 compared to saline by two-sample t-test. **C–D.** Spearman correlation analysis of the relationship between inflammation and mean blood vessel density in the DLP of the saline and *E. coli* infected adult male mice at day 3 **(C)** and 7 **(D)** post-instillation. PID Post instillation day.

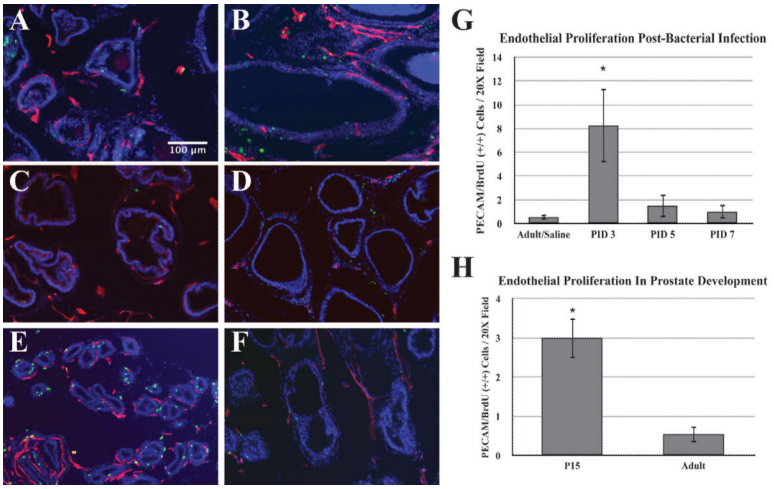

Figure 5.

A–F. Immunostaining for BrdU (Green), PECAM (Red) and DAPI (Blue) in the adult prostate of saline-instilled control **(A)**, 3 days post-bacterial inoculation **(B)**, 5 days post-bacterial inoculation **(C)**, 7 days post-bacterial inoculation **(D)**, postnatal day 15 **(E)** and adult **(F)** prostate. Scale bar 100μm. **G.** Comparisons of the endothelial proliferation determined by double positive PECAM/BrdU (+/+) cells per 20X field in the prostate after saline instillation (n=5) and day 3, 5, 7 post-bacterial inoculation (n=4 each time point). The data are presented as the mean ± SEM. * indicates p-value < 0.05 compared to saline by two-sample t-test. **H.** Comparison of endothelial proliferation determined by double positive PECAM/BrdU cells per 20X field in the prostate of postnatal day 15 (n=6) and adult (n=6) male mice. The data are presented as the mean ± SEM. * indicates a p-value < 0.05 compared to adult by two-sample t-test. PID Post instillation day.

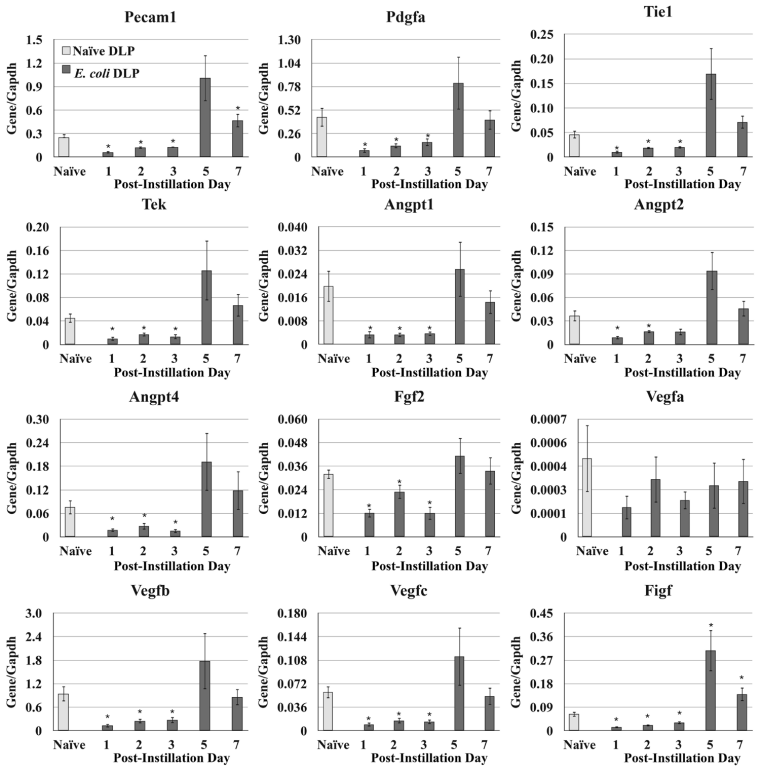

Figure 6.

qRT-PCR for the angiogenic factors in the DLP of the naïve and *E. coli* infected adult male mice at day 1, 2, 3, 5, and 7 after instillation. The data are presented as the mean ± SEM. * indicates p-value < 0.05 compared to naïve by two-sample t-test. PID post instillation day.

TABLE I

Primer Sequences (5' to 3') Used for RT-PCR Analysis

Mediator	Forward Sequence	Reverse Sequence
Pecam1	GTCAGAGTCTTCCTTGCCCC	CTGTTTGGCCTTGGCTTTCC
Pdgfa	AGTCAGATCCACAGCATCCG	TGGTTAATGGCATGGGACCC
Tie1	GCTGCTCCCCACTCTTTTCT	GACACGCAGGTCAGGAAGAA
Tek (Tie2)	ACCTCTTGTGTCTGATGCCG	CAGTGGATCTTGGTGCTGGT
Angpt1	TTCTTCCAGAACACGACGGG	AAGAGAAATCCGGCTCCACG
Angpt2	CATAGCAGCCCCTTTCCACA	GACTGCAGTGCCTTTGGTTG
Angpt4	GGTAATGTGGCCAGAGAGCA	TCCCAGTCATGCAGTTCCAC
Fgf2	GAGAAGAGCGACCCACACG	CAGCCGTCCATCTTCCTTCA
Vegfa	ACTTCTGAGGGGCCTAGGAG	AGGTGGGGTAAGGAGAGGAC
Vegfb	GTGCCTCTGAGCATGGAACT	ACATTCCAGGCCATCGTCAG
Vegfc	CAGCCCACCTCAATACCAG	CTCACGTGGCATGCATTGAG
Figf (Vegfd)	CCCATCGCTCCACCAGATTT	CGCATGTCTCTCTAGGGCTG
Gapdh	AGAACATCATCCCTGCATCC	CACATTGGGGGTAGGAACAC